

Comparative study of velocities under hydrostatic and non-hydrostatic stress in sands

Sandra Vega*, Manika Prasad, and Gary Mavko
Stanford Rock Physics Laboratory

Summary

In this paper, we compare V_p measured under hydrostatic and non-hydrostatic stress conditions in a sand. We describe how we apply isotropic stress using a polyaxial apparatus. We examine velocities in three perpendicular directions as function of stress and find that V_p under hydrostatic pressure is higher than V_p measured under non-hydrostatic isotropic stress. Furthermore, we observe that velocity anisotropy revealed the intrinsic anisotropy in the sands.

Introduction

Laboratory measurements of acoustic velocity in sands are most often made under hydrostatic pressure (Domenico, 1997; Zimmer et al., 2002; Wang, 2002). Stresses in the lithosphere are generally non-hydrostatic and anisotropic (Sinha and Kostek, 1996; Winkler et al., 1994; Zoback and Zoback, 2000). Although Mavko et al. (1995) suggested a method for rocks to predict velocity anisotropy in an anisotropic stress from hydrostatic lab measurements of V_p and V_s , a similar prediction for sands is not yet well understood.

Domenico (1977) measured acoustic velocities under hydrostatic pressure in a sand and in glass beads of similar grain size and porosity. The velocity, pore volume, porosity, and pore compressibility as functions of pressure found for the dry and brine saturated sample are useful for a better understanding of unconsolidated formations. Wang (2002) measured velocity anisotropy under hydrostatic pressure in the lab on sands, shales, and rocks. A relation to estimate V_p anisotropy from V_s anisotropy and vice versa was found. However, as all these correlations have been measured under hydrostatic pressure, they have to be carefully extrapolated to in situ stress.

In this paper, we present an experimental study of velocity measurements in sands at isotropic stress condition in a hydrostatic oil-loading system and a polyaxial piston-loading system. We compare velocities measured under these two conditions and show that they are not equal. This is the first step toward a better understanding of how to relate velocities measured under hydrostatic pressure and in situ stress velocities in sands.

Experimental setup and procedure

We used a hydrostatic and a polyaxial apparatus to compare compressional velocity (V_p) and strain (ϵ) under

hydrostatic and non-hydrostatic stress in a sand. We implemented a test called quasi-hydrostatic which consists of creating isotropic stress ($\sigma_z \approx \sigma_x \approx \sigma_y$) in the polyaxial apparatus.

Quasi-hydrostatic test

For the quasi-hydrostatic stress test, we adapted a polyaxial apparatus (Yin, 1993) to make V_p and ϵ measurements in unconsolidated materials (Vega et al., 2003). In this apparatus the sample is contained in an aluminum cell that can be loaded in three orthogonal directions with pistons.

In the quasi-hydrostatic stress test, the same stress was applied in all three directions, $\sigma_z \approx \sigma_x \approx \sigma_y$. We loaded (and unloaded) the samples by successively incrementing σ_z , then σ_x , and following with σ_y . To check the possible influence of loading sequence on the results, we also changed the order of loading increments to σ_x , σ_y , and then σ_z . We waited after the first stress increment eight to ten hours before starting the V_p and ϵ measurements. At each step, we followed the same order of loading (and unloading) and the stresses were allowed to stabilize (average about half an hour) before making the acoustic measurements.

Hydrostatic test

For the hydrostatic stress tests, we used an oil-loading pressure vessel (Vanorio et al., 2002). The sample is contained in a cylindrical tygon jacket and is subjected to a confining pressure generated with oil.

In order to be consistent with the polyaxial test, the confining pressure steps were the same as in the quasi-hydrostatic test and the sample was allowed to stabilize (average about half an hour) before making the acoustic measurements. The principal frequency of the piezoelectric crystals for P-wave generation was 1 MHz in both apparatus.

Samples and sample preparation

We used a beach sand with an average grain size of 0.25 mm and grain density 2.060 g/cc. The grain size analysis was made by sieving, and the grain density was measured using a pycnometer. This sand shows natural stratification when it is poured (Figure 1a). Natural stratification has also been observed in different mixtures of granular materials (Makse et al., 1997; Baxter et al., 1998; Cizeau et al., 1999).

Comparative study of velocities under hydrostatic and non-hydrostatic stress in sands

We made four sand samples, one for the hydrostatic test, HNS, and three for the quasi-hydrostatic test QNS1, QNS2, and QRS. All samples were poured in the vertical direction (Z) creating the natural stratification characteristic of this sand. The HNS sample was poured in a cylindrical rubber jacket for the hydrostatic apparatus and the QNS samples were poured into the aluminum cell for the polyaxial apparatus. QRS was first poured and then rotated 90° around the X-axis, i.e. Z and Y directions were exchanged in the final configuration (Figure 1b). For the hydrostatic apparatus, a sample similar to QRS was not possible due to limitations of the setup. The samples were flattened by tamping for a better transducer-sample coupling.

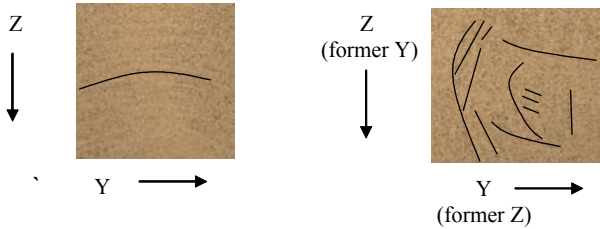


Figure 1: (a) Natural stratification shown in the poured sand: the black line shows one of the layers naturally formed. (b) Rotated sand around X direction, equivalent to the QRS sample: the black lines show mainly interpreted features. (Pictures taken in a transparent container outside the aluminum cell).

Initial porosity (ϕ) was calculated from the volume and grain density of the sand samples. Average porosity was 47% with a sample-to-sample error lower than 2% (Table 1). All samples were measured dry during the loading and unloading of three stress cycles up to 40 bars. In this paper, we show the loading path of the first cycle as velocity and strain results did not reveal a significant hysteresis. QNS1 was used for the Z→X→Y loading order, and QNS2 for the X→Y→Z loading order. Table 1 summarizes the general characteristics of the samples.

Table 1: Sample summary

Sample name	Test*	Fabric**	Loading order	ϕ
HNS	H	NS		46.1
QNS1	Q	NS	Z→X→Y	47.9
QNS2	Q	NS	X→Y→Z	46.8
QRS	Q	RS	Z→X→Y	47.3

* H: hydrostatic, Q: quasi-hydrostatic

** NS: natural stratification, RS: rotated stratification

Results

Fabric anisotropy

Figure 2 and Figure 3 show V_p as a function of the mean stress, $\sigma = (\sigma_z + \sigma_x + \sigma_y) / 3$, for QNS1 and QRS, respectively. Figure 2 displays the velocity anisotropy in QNS1 due to its depositional anisotropy. V_{pz} , which was in the perpendicular direction to the layering, was lower than V_{px} and V_{py} , as in a typical TI medium. A change in the loading direction (QNS2) produced similar results. To test whether the sample had textural anisotropy, we measured velocity in a rotated cell, QSR (Figure 3). Velocity in the unchanged horizontal direction V_{px} remained high. However, velocities in the exchanged vertical (V_{pz}) and horizontal (V_{py}) directions were now equal and lower than V_{px} .

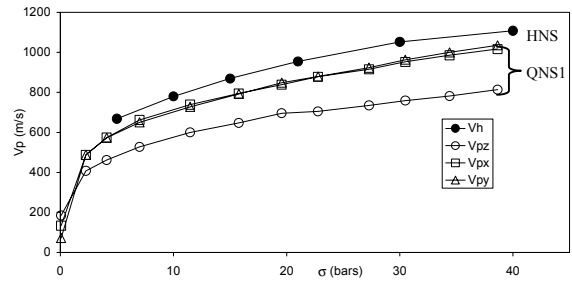


Figure 2: Velocity as a function of stress for sample QNS1. Open circles, squares, and triangles denote QNS1 V_{pz} , V_{px} , and V_{py} , respectively. Close circles represent HNS velocity in the Z direction, V_h .

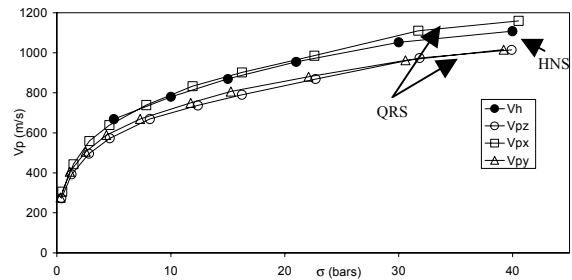


Figure 3: Velocity as a function of stress for sample QRS. Open circles, squares, and triangles denote QRS V_{pz} , V_{px} , and V_{py} , respectively. Close circles represent HNS velocity in the Z direction, V_h .

Figure 4 shows strain in the Z direction (ϵ_z) as a function of the stress for all samples. We found the same trend ϵ_z - σ for the samples measured in the polyaxial apparatus, and a slightly different trend for the HNS sample. The strain for QRS was higher than for QNS samples, which must be influenced by the fabric anisotropy as the sample-to-sample porosity difference was relatively small (0.5-0.6%). In

Comparative study of velocities under hydrostatic and non-hydrostatic stress in sands

addition, there was a difference between the strain of QNS1 and QNS2 that is most likely a consequence of the porosity, which varied by 1.1% between these samples.

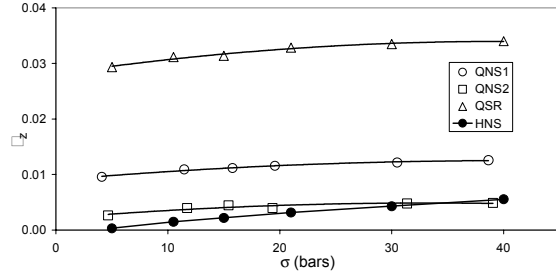


Figure 4: Strain measured in the quasi-hydrostatic test as a function of the strain measured in the hydrostatic test. Symbols denote measured values, solid lines represent second order polynomial fits.

Vp under hydrostatic and non-hydrostatic stress

Figure 2 shows V_p in the Z direction for HSN (V_h) as a function of pressure, and it is compared with the QNS1 velocities. As revealed by the graph, V_h was higher than the QNS1 velocities. We can also see that the V_h -pressure curve increases faster than the V_{pz} -stress curve for QNS1 at stresses lower than 22 bars, and increases slower at stresses higher than 22 bars.

Figure 3 shows V_h as a function of the pressure, and it is compared with the QRS velocities. As for QNS1 in Figure 2, V_h was also higher than the velocities in the Z direction. The V_h -pressure curve and V_{pz} -stress curve for QRS increase equally at stresses lower than 22 bars, and the V_h -pressure curve increases slower than this V_{pz} -stress curve at stresses higher than 22 bars.

Table 2 summarizes the velocity comparison between the samples under hydrostatic and non-hydrostatic stress. It is clear that velocities measured under hydrostatic pressure are not equal to velocities measured under non-hydrostatic stress fields, even for an approximately isotropic stress field with the same fabric anisotropy (HNS, QNS1, and QNS2).

Table 2: Velocity comparison summary

Sample	Velocities		$\frac{V_h - V_z}{V_h}$	$\frac{V_h - V_x}{V_h}$
	Same direction	Different direction		
HNS QNS1 QNS2	$V_h > V_{pz}$	$V_h > V_{px} \approx V_{py}$	27%	7% - 12%
HNS QRS	$V_h > V_{pz}$	$V_{px} \geq V_h > V_{py}$	8% - 12%	4%

Discussion

Fabric anisotropy

The velocity anisotropy detected in QNS1 (Figure 2) and QNS2 is consistent with the natural stratification shown in Figure 1a. The velocity anisotropy detected in QRS (Figure 3) deviates from a TI anisotropy. For instance, Figure 1b shows that the packing of QRS is more complex than QNS. For QRS, it seems that some of the original layers formed during pouring became more curved after the rotation due to gravity. In a simple way, this can explain why V_{pz} and V_{py} are lower than V_{px} . V_{py} is measured in the perpendicular direction to the layers, V_{pz} is perpendicular to the layer edges, and V_{px} is in the direction of the still parallel layers.

V_h was higher than V_{pz} for the two packings, QNS and QRS. It was 27% higher for QNS, and 8-12% for QRS (Table 2). This difference between QNS and QRS indicates that the divergence between velocities measured under hydrostatic and non-hydrostatic conditions can be also affected by the fabric anisotropy of the sands. Therefore, it must be necessary to know the direction of the velocity measurement with respect to the geological formation anisotropy to extrapolate hydrostatic lab V_p to non-hydrostatic in situ V_p .

Vp under hydrostatic and non-hydrostatic stress

In order to see if there is a correlation between velocities measured under hydrostatic pressure and quasi-hydrostatic stress, we plotted V_{pz} as a function of V_h for all samples with same fabric anisotropy (Figure 6). As revealed by the graph, the samples have the same trend.

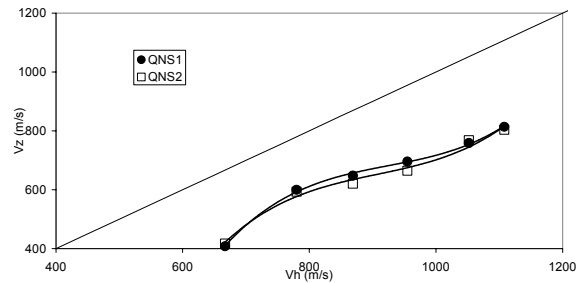


Figure 6: Compressional velocity measured in the quasi-hydrostatic test as a function compressional velocity measured in the hydrostatic test.

In order to check edges effects in the polyaxial apparatus, we evaluated the stress in the borders of the cell using a surface line load on a semi-infinite solid region approximation (Jaeger and Cook, 1979). We found that stress at the edges were approximately 2% lower than the

Comparative study of velocities under hydrostatic and non-hydrostatic stress in sands

applied stress. However, the relative difference between V_h and V_{pz} changes less than 1% when this edge stress effect is added.

Conclusions

The velocity anisotropy under isotropic stress revealed intrinsic anisotropy in the sand samples. Moreover, V_p measured under hydrostatic pressure was higher than V_p measured under non-hydrostatic stress in the sand, for the same fabric anisotropy and similar isotropic stress. The difference between hydrostatic V_p and non-hydrostatic V_p was not due to border effects in the semi-infinite solid approximation. Nevertheless, line forces in granular material are non-uniform and might affect the velocity-stress results. Further work is required to fully explain the results found in this paper.

References

- Baxter, J., Tuzun, U., Heyes, D., Hayati, I., and Fredlund P., 1998, Stratification in poured granular heaps, *Nature*, 391, 136.
- Cizeau, P., Makse, H. A., and Stanley, E., 1999, Mechanisms of granular spontaneous stratification and segregation in two-dimensional silos, *Physical Review E*, 59, 4408-4421.
- Domenico, S. N., 1977, Elastic properties of unconsolidated porous sand reservoirs: *Geophysics*, 42, 1339-1368.
- Geng, J., Howell, D., Longhi, E., and Behringer, R. P., 2001, Footprints in sand: the response of a granular material to local perturbations: *Physical Review Letters*, 87, 0355061-0355064.
- Jaeger, J. C., and Cook, N. G. W., 1979, *Fundamentals of Rock Mechanics*, Halsted Press, New York.
- Mavko, G., Mukerji, T., Godfrey, N., 1995, Predicting stress-induced velocity anisotropy in rocks: *Geophysics*, 60, 1081-1087.
- Sinha, B. K. and Kostek, S., 1996, Stress-induced azimuthal anisotropy in borehole flexural waves: *Geophysics*, 61, 1899-1907.
- Vanorio, T., Prasad, M., Nur, A., and Patella, D., 2002, Ultrasonic velocity measurements in volcanic rocks: correlation with microtexture: *Geophysical Journal International*, 149, 22 - 36.

Vega, S., Prasad, M., Mavko, G., and Nur, A., in preparation, Stress-induced velocity anisotropy in sands: preliminary results: *Geophysical Research Letters*.

Wang, Z., 2002, Seismic anisotropy in sedimentary rocks, part 2: laboratory data: *Geophysics*, 67, 1423-1440.

Winkler, K., Plona, T., Hsu, J., and Kostek, S., 1994, Effects of borehole stress concentrations on dipole anisotropy measurements: 64th Annual International Meeting, Society of Exploration Geophysicists, Expanded Abstracts, 1136-1138.

Yin, H., 1993, "Acoustic velocity and attenuation of rocks; isotropy, intrinsic anisotropy, and stress-induced anisotropy": Ph.D. Thesis, Stanford University, Stanford, CA.

Acknowledgments

We thank the SRB consortium and the U.S. Department of Energy for their support to this research.